NASA CR - 66400

SOME MODIFICATIONS OF SIMPLE DESCRIPTIONS OF YIELDING AT CRACK TIPS

Bill R. Baker
Stanford Research Institute
Menlo Park, California

May 26, 1967

Contract No. NAS 1-5885

Project No. 5958

Report No. 3

Prepared for

National Aeronautics and Space Administration
Langley Research Center
Langley Station
Hampton, Virginia

ABSTRACT

Modifications of the Dugdale model are introduced which eliminate the discontinuous transverse displacement at the end of the crack and permit the satisfaction of a Mises yield condition at the crack tip. Calculations are made to obtain additional points on the elastic-plastic interface near the crack. Suggestions are made for introducing work-hardening properties of the material.

I INTRODUCTION

The first theoretical investigation of the stability of cracks in a loaded structural element was made by Griffith [1]. He utilized the analysis of Inglis [2] for a cracked elastic plate subjected to tension in order to formulate a stability criterion. The results were so simple that they remain quite popular even though the solution yields stress components which are singular at the crack tips. Correspondingly, the initially parallel edges of the crack are wrenched apart and rotated through a relative angle of π at the crack tips.

These singularities of stresses were finally eliminated in works by Christianovitch [3], Barenblatt [4], and Dugdale [5]. In all three of these investigations the solutions are still obtained from the linear theory of elasticity, but other loads in addition to the uniform stress field at infinity are acting to cancel the fundamental singularities. In the example considered by Christianovitch the pressure of a liquid which partially wets the surface of a crack is balanced against an external compressive stress acting far from the crack. Barenblatt has introduced the concept of cohesive forces acting in a very small end zone of the crack which resist the applied loads. This model is very useful for the description of brittle materials while the model of Dugdale is applicable to very ductile materials. The latter model provides a simple representation of the forces exerted by the plastically deformed material at the crack tips. However, the Dugdale model does not give a criterion for the ultimate strength of a cracked panel.

In the present report some refinements are suggested. Although some of the properties of the plastically deformed regions are considered,

it is found that additional information can be obtained from simple solutions from the theory of linear elasticity.

In his original model, Dugdale replaced the very complicated non-linear problem of the growth of plastic regions at crack tips by a simpler linear elastic problem with new boundary conditions.

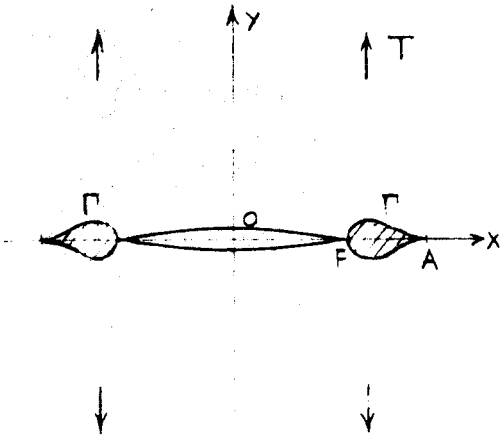

Fig. 1

PLASTIC REGIONS IN A THIN PLATE OF DUCTILE MATERIAL

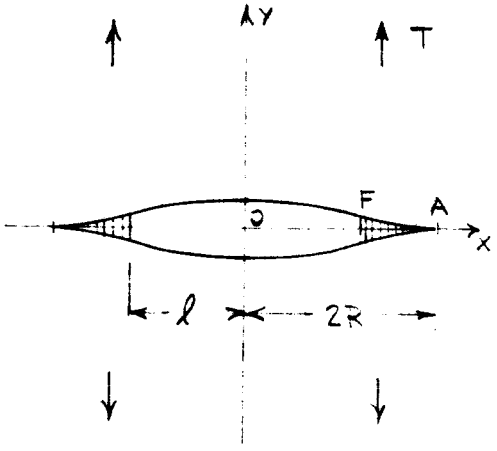

Fig. 2

DUGDALE'S REPRESENTATION

Dugdale observed experimentally that if the plate is rather thin and if the material is very ductile then the yielded zones are quite narrow and have the shape indicated by curves Γ in Fig. 1. He therefore established a comparatively simple, but very useful, model as indicated in Fig. 2. In the mathematical model the slit is extended straight through the plastic region out to the point A. The fact that yielding has occurred inside the curve Γ is replaced by the following conditions. The infinite elastic plane is artifically extended right up to the x-axis. Boundary conditions are not specified on the actual interface Γ but they are given on the segment FA, which will be called yield segment here in contrast to the

yield zone. The value of the normal stress on the yield segment is taken to be Y_s, the yield stress in simple tension, and the length of the yield segment is adjusted with respect to the real crack length 2ℓ and the applied tensile stress T so that stresses are finite (and continuous) at point A. The simple relation obtained by Dugdale is

$$\frac{T}{Y_s}\frac{\pi}{2} = \text{arc cos } \left(\frac{\ell}{2R}\right) \tag{1}$$

Dugdale's experiments show that the length of the yield zone agrees remarkably well with equation (1). Similar experiments by Rosenfield, Dai and Hahn [6] and by Forman [7] also agree with Dugdale's results. However, the result (1) does not define a critical stress for rupture at the crack tip. In the next section we will consider some refinements which must be made before a failure criterion can be introduced.

II DISPLACEMENTS AND STRAINS AT THE CRACK TIP FOR THE DUGDALE MODEL

It would be desirable to be able to determine the critical stress level T which causes failure in a cracked plate of a material with given yield stress and strain-hardening characteristics. This suggests that a certain measure of strain at the crack tip might be the proper quantity to use in a failure criterion. This question was considered by Goodier and Field [8], who noted that the solution of the problem posed by Dugdale leads to a discontinuity of transverse displacement, v, at the end F of the real crack. The vertical displacement of the edges of the slit are indicated in Fig. 2 in a greatly exaggerated scale. The finite stress condition (1) does assure that the ends of the slit close smoothly at A but the sides actually open between F and A as is indicated by the cross hatching. Therefore it is not possible to use the usual definitions to discuss the transverse strains on the yielded segment. As an alternative measure of the strain, Goodier and Field proposed that there exist some "gage length" d and then the "critical strain" can be defined as the ratio of the vertical displacement at F divided by the gage length, i.e.,

$$\epsilon_{\text{critical}} = \frac{v_F}{d} \tag{2}$$

Although this does give a "strain" which has the correct dimensions and which increases monotonically with the load T, it is not clear how this can be related to other tests such as a simple tension test to determine a critical load for the cracked plate.

Rosenfield, Dai, and Hahn did modify the normal stress acting on the segment FA so that the stress corresponds to a local transverse strain defined as in (2). These authors replaced the constant normal stress of Dugdale's model with a piecewise constant distribution of normal stresses.

The stress on each segment was set equal to the stress measured in a simple tension test at the same value of strain. However, since it was not possible to define the gage length, the results remain a bit indefinite.

We will now consider some improvements of Dugdale's model which are necessary for the definition of a critical strain. Additional consideration will be given to the coupling between the elastic portion of the plate and the plastically deformed material within the yield zones bounded by the curves Γ in Fig. 1. Although the elastic region really is bounded by the interface curve Γ, it is convenient to represent the solution in terms of an elastic plane which is continued across Γ up to the real axis just as in Dugdale's formulation. This formulation is chosen because it is still impossible to solve the plane elasticity problem for data given on an arbitrary contour such as Γ, but the complex variable methods can be used effectively for the plane with a slit. Eventually it will be desirable to satisfy certain boundary conditions on the curve Γ but it is possible to do that by modifying the stresses on the segment FA of the slit plane. Now we will consider application of different loads to the segment FA, and we begin with modification of the normal load.

III MODIFICATION OF NORMAL LOADS

In order to achieve a definition of strain near the crack tip which will be compatible with any continuum theory it is necessary to at least eliminate the jump in vertical displacement across the slit at point F. Simple solutions of the loading of an interval of the edge of a half-plane by a constant pressure shows that if the resultant force is held constant as the length of the interval shrinks, then the local displacement can be made very large, see Muskhelishivili [9], Section 93. Therefore, we expect that the displacement v_F can be eliminated by adding more tensile stress near the point F.

Basic solutions of the type used by Dugdale can be superposed to obtain an arbitrary step-wise constant distribution of stresses on the yield segment, FA, in the manner of Rosenfield, Dai, and Hahn. An example with five steps is sketched in Fig. 3.

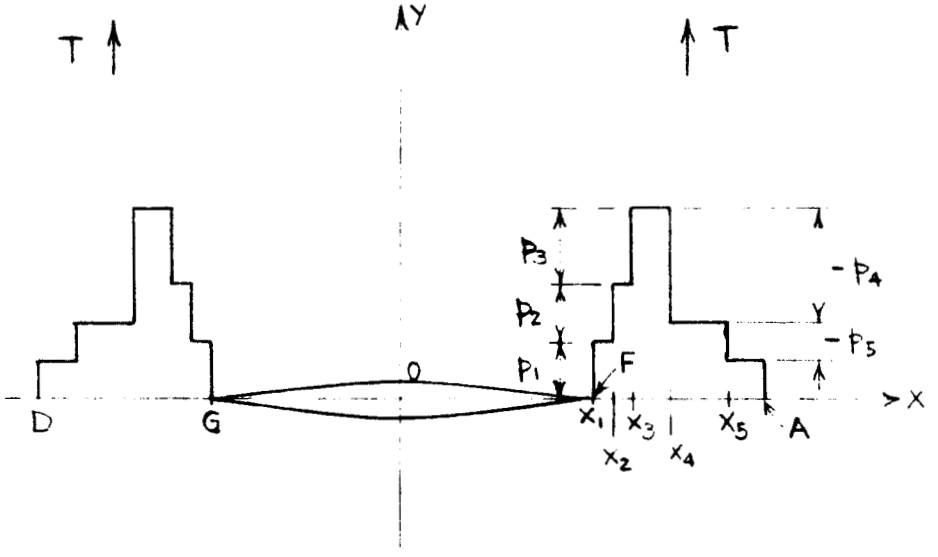

Fig. 3

STEP-WISE CONSTANT DISTRIBUTION OF NORMAL STRESS ON THE YIELD SEGMENT FA

The calculations of stresses and displacement are simplified if the simple state of compression $\sigma_y \equiv -T$, $\sigma_x \equiv \tau_{xy} \equiv 0$ is first added to the problem sketched above. Then all stress components tend to zero at infinite distance from the crack.

Methods for the solution of the first fundamental problem of an elastic plate containing an elliptical hole are given in the books of Muskhelishvili and Sokolnikoff [10]. We will use the notation of Sokolnikoff here and consider the limiting case of a flattened ellipse or slit. However, to illustrate the types of loads and to discuss the mapping, it is more convenient to sketch an elliptical hole in the physical or z-plane and keep in mind that our analytical results have been specialized to the flattened ellipse. The basic problem of a single step in normal load is sketched in Fig. 4.

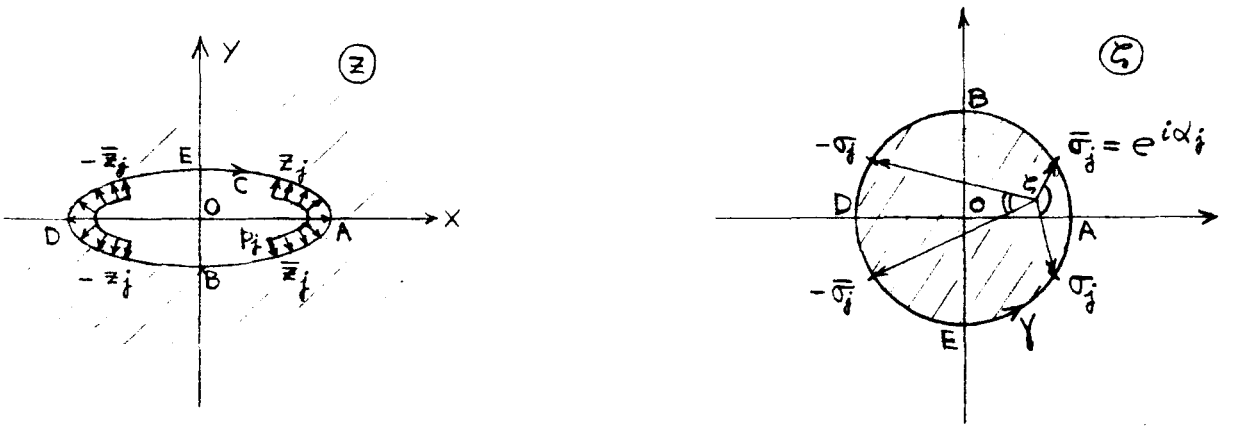

Fig. 4

THE ELLIPSE BEFORE FLATTENING TO A SLIT
AND ITS MAP IN THE ζ-PLANE

The first step of the analysis is to map the exterior of the hole of the z-plane onto the unit circle in the ζ-plane. The transformation for the general elliptical hole is

$$z = \omega(\zeta) = R\left(\frac{1}{\zeta} + m\zeta\right) \tag{3}$$

The boundary of the elliptical hole is denoted by C, and the positive direction on C is clockwise so that the elastic region lies on the left. Correspondingly, the positive direction on the boundary γ in the ζ-plane is counterclockwise. The point z_j in the first quadrant at the end of the step of normal pressure in the z-plane is mapped into σ_j in the fourth quadrant on the unit circle γ. The map of the conjugate point $\overline{z_j}$ on the lower edge of the ellipse goes into $\overline{\sigma_j} = e^{i\alpha_j}$.

In Appendix A the solution for the stress potentials is discussed more fully, and here we will consider some results for the slit where $m = 1$ in the mapping function (3). The stress components are obtained from the formulas

$$\sigma_x + \sigma_y = 4\mathrm{Re}\left\{\frac{-p_j}{2\pi i}\left[L_{4j}(\zeta) + \frac{4i\alpha_j}{\zeta^2-1}\right]\right\} \tag{4a}$$

$$\sigma_y - \sigma_x + i2\tau_{xy} = \frac{-p_j}{\pi i}\frac{\zeta^2}{\zeta^2-1}\left\{(\bar{\zeta} + \frac{1}{\zeta})\left[L'_{4j}(\zeta) - \frac{8i\alpha_j\zeta}{(\zeta^2-1)^2}\right] + \frac{8i\alpha_j}{1-\zeta^2} + \frac{16i\alpha_j\zeta^2}{(1-\zeta^2)^2} - \frac{z_j}{R}L'_{3j}(\zeta)\right\} \tag{4b}$$

where the functions $L_{3j}(\zeta)$ and $L_{4j}(\zeta)$ are

$$L_{4j}(\zeta) \equiv L_{1j}(\zeta) + L_{2j}(\zeta) \qquad L_{3j}(\zeta) \equiv L_{1j}(\zeta) - L_{2j}(\zeta)$$

$$L_{1j}(\zeta) \equiv \ln\frac{\bar{\sigma}_j - \zeta}{\sigma_j - \zeta} \qquad L_{2j}(\zeta) \equiv \ln\frac{-\bar{\sigma}_j - \zeta}{-\sigma_j - \zeta} \tag{5}$$

and the imaginary parts of the last functions are positive with

$$0 \leq \mathrm{Im}L_{1j},\ \mathrm{Im}L_{2j} < 2\pi \tag{6}$$

The positive angles which are marked in the unit circle of Fig. 4 represent the imaginary parts of L_{1j} and L_{2j}.

Closer examination of equations (4a) and (4b) shows that the stresses do tend to zero as $\zeta \to 0$ (or $|z| \to \infty$) but there is a singularity at $\zeta = \pm 1$ due to the terms which are directly proportional to α_j. This corresponds, for example, to a square root singularity of the order $(z - 2R)^{-1/2}$ at the right hand end of the slit in the z-plane. The original solution of Inglis which was used by Griffith to establish his energy criterion for crack growth can be obtained by setting

$$\alpha_j = \alpha_0 = \frac{\pi}{2}, \qquad p_j = p_0 = T \tag{7}$$

in equations (4a) and (4b).

In order to eliminate the singularity of the Inglis solution, Zheltov and Christianovich and Dugdale added one more term due to a step load. Dugdale chose

$$p_1 = -Y_s \qquad \alpha_1 = \frac{T}{Y_s}\frac{\pi}{2} \tag{8}$$

which results in equation (1).

As Rosenfield, Dai, and Hahn noted, it is possible to superpose N+1 steps and obtain finite stresses at point A if the following finiteness condition is enforced

$$\sum_{j=0}^{N} p_j \alpha_j = 0 \tag{9}$$

The stress components due to the steps in normal load are obtained by summing over j from 0 to N in equations (4a) and (4b), and all linear terms in the α_j cancel because of the finiteness condition (9). The applied load is

$$T = p_0 = -\frac{2}{\pi}\sum_{j=1}^{N} p_j \alpha_j \tag{10}$$

The state of simple tension must be added to return to the original problem indicated in Fig. 3. This simple tensile field can be modified by rigid body motions so that $v(x,0) \equiv 0$, and hence the vertical displacement at F depends only on the various step loads.

In Appendix A it is shown that the contribution of the j^{th} step load to the vertical displacement at the edge of the slit is

$$\frac{v}{R}\,2\mu = -p_j \frac{1+\kappa}{2\pi}\left\{\cos\theta\,\ln\frac{\sin^2(\alpha_j+\theta)}{\sin^2(\alpha_j-\theta)} + \cos\alpha_j\,\ln\frac{(\sin\alpha_j-\sin\theta)^2}{(\sin\alpha_j-\sin\theta)^2}\right\} \equiv -p_j V_{nj}(\theta) \qquad (11)$$

The elastic constant κ for the case of generalized plane stress can be expressed in terms of Poisson's ratio υ:

$$\kappa = \frac{3-\upsilon}{1+\upsilon} \qquad (12)$$

Dimensionless loads c_j will now be introduced where

$$c_j \equiv -\frac{p_j}{Y_n} \qquad (13)$$

and Y_n is an arbitrary reference stress for the normal loads. A boundary point $\zeta = e^{i\theta}$ in the ζ-plane goes into the following point on the slit

$$x = 2R\cos\theta, \qquad y = 0 \qquad (14)$$

The end of the real crack corresponds to $\theta = \pm\alpha_1$ so the displacement conditions at F can be written in terms of the functions of (11).

$$\sum_{j=0}^{N} c_j V_{nj}(\alpha_1) = 0 \qquad (15)$$

This condition as well as the finiteness condition (9) can be satisfied if $N \geq 2$.

In general the opposite sides of the slit will overlap along the yield segment FA, but this is acceptable since we are establishing an elastic

solution which is valid only outside the curve Γ. However, from elementary considerations of both the elastic and the plastic regions near point F we can conclude that the slope of the real crack must also vanish at F.

From the symmetry of the real plastic region it follows that the shear stress, τ_{xy}, and the vertical displacement, v, are identically zero on the x-axis. Hence, if we assume that the strain-hardening is orthotropic, that is, the directions of principal stresses and principal strains coincide, then the shear strain, γ_{xy}, must also be zero on the plastic side of Γ at F. Of course, the shear stress, τ_{xy}, and consequently the strain, γ_{xy}, are also zero on the elastic side of F so the real crack must close with zero slope at F. This slope condition can also be expressed in terms of the displacement functions (11).

$$\sum_{j=0}^{N} c_j \frac{dV_{nj}}{d\theta}(\alpha_1) = 0 \tag{16}$$

Since the term $\frac{dV_{n1}}{d\theta}(\theta)$ has a logarithmic singularity at $\theta = \alpha_1$, it follows that we must choose

$$c_1 = 0 \tag{17}$$

It is useful now to briefly consider the yield condition on the elastic plastic interface. It will be assumed that a Mises yield condition holds in the plastic region, and for our case of plane stress it can be written

$$f \equiv 3(J_2 - k^2) = \sigma_x^2 - \sigma_x\sigma_y + \sigma_y^2 + 3\tau_{xy}^2 - 3k^2 = 0 \tag{18}$$

In general the term k^2 depends on the plastic strain history, but for initial yielding or points on the elastic-plastic interface, $\sqrt{3}k$ can be taken to be the simple tensile yield stress Y_s so that

$$f = \sigma_x^2 - \sigma_x\sigma_y + \sigma_y^2 + 3\tau_{xy}^2 - Y_s^2 = 0, \text{ on } \Gamma \tag{19}$$

The curve Γ passes through the point F at the end of the free surface of the real crack so two of the stress components vanish at F and we find

$$\sigma_{yF_-} = \tau_{xyF_-} = 0, \qquad \sigma_{xF_-} = Y_s \tag{20}$$

where the subscript F_- denotes the limiting value from the left.

Now we would like to adjust the coefficients c_j of the basic normal load solutions so that condition (20) would be satisfied. However, this is impossible because of the following result which can be obtained from Secion 93 of Mushkelishvili's book or from careful inspection and superposition of solutions of the type given in equations (4a) and (4b).

The two stress components σ_x and σ_y are equal at a point on the edge of an elastic half-plane $y \geq 0$ if

a. The shear stress τ_{xy} vanishes on $y = 0$,

b. All stress components are of order $o(\frac{1}{z})$ as $|z| \to \infty$, and

c. The component σ_y is continuous at the point of observation.

A statement of this type was made by Goodier and Field except that conditions b and c were omitted. The state of simple tension $\sigma_y \equiv T$, $\sigma_x \equiv \tau_{xy} \equiv 0$ would not be excluded if b were left out, and c is necessary if we are to discuss values at a point. These seemingly fine details are of importance at the point F which is a point of discontinuity in the Dugdale solution. However, the condition (17) results in continuity of σ_y at F for the present solution.

The conditions a and b are satisfied by each of the basic step loads so equality of σ_x and σ_y on the slit follows except at the point of discontinuity, $\theta = \alpha_j$. Only the zeroth step load gives a contribution at $\theta = \alpha_1$, and we find

$$\sigma_{xF} = \sigma_{yF} = -p_0 = -T \tag{21}$$

Addition of all other steps of normal load and of the state of simple tension does not change the value of σ_{xF}. Consequently the yield condition (20) can never be satisfied by a combination of normal loads. This leads us to consider the addition of tangential loads on the yield segment.

IV TANGENTIAL LOAD

The distribution of shear stresses will also be taken as a finite sum of steps in tangential load of the kind illustrated in Fig. 5.

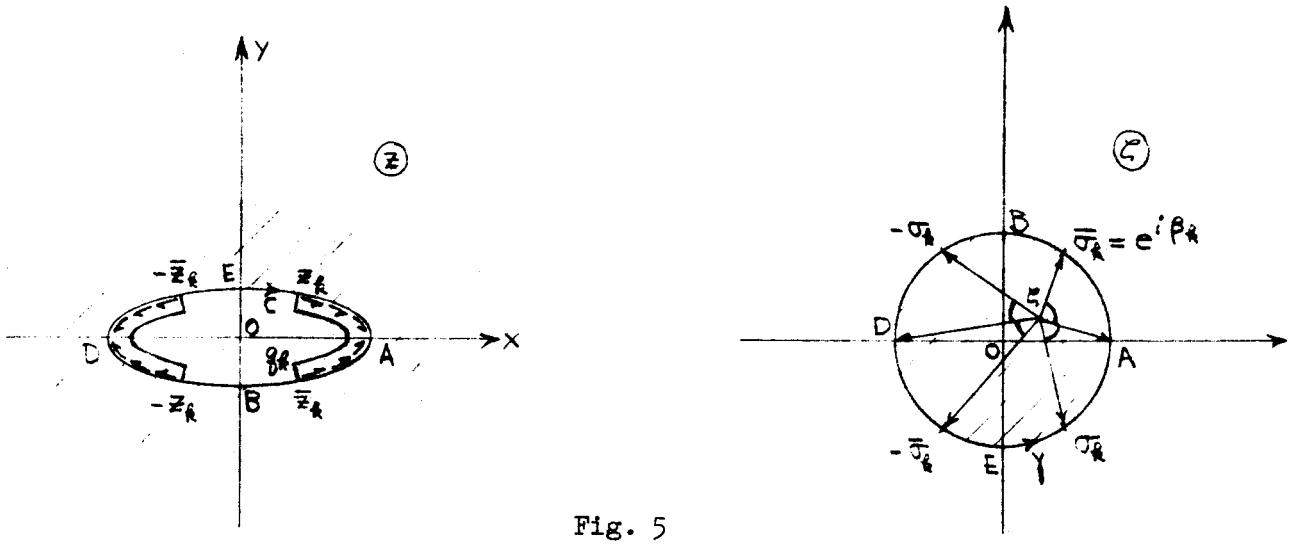

Fig. 5

THE STEP TANGENTIAL LOAD

Tangential loads of intensity q_k act in directions away from the y-axis so the shear stress at the boundary alternates in sign between successive quadrants. The point z_k at the end of the stress free arc maps into

$$\sigma_k = e^{-i\beta_k}$$

Calculations described in Appendix A result in the following stress components for the typical k^{th} load.

$$\sigma_x + \sigma_y = \frac{2q_k}{\pi} \mathrm{Re}\{L_{58k}\} \tag{22}$$

$$\sigma_y - \sigma_x + i2\tau_{xy} = \frac{q_k}{\pi}\left\{-2L_{58k} + \frac{\zeta}{\zeta^2-1}\left[\zeta(\bar{\zeta} + \frac{1}{\bar{\zeta}}) - \zeta^2 - 1\right]L'_{58k}\right\} \tag{23}$$

where the logarithmic function L_{58k} is defined in Appendix A. As in the case of normal loads we find that any single step distribution of tangential loads leads to a stress singularity at the end of the slit. However, for this case the singularity is of the logarithmic type in the stress component τ_{xy}.

Detailed expansions about the points $\zeta = \pm 1$ show that the dominant terms are directly proportional to q_k so it is possible to obtain a finite stress at A by superposing several step loads such that

$$\sum_{k=1}^{M} q_k = 0 \tag{24}$$

This simply means that the total shear stress at the end of the slit is zero.

An additional condition can be derived from the fact that the resultant of all forces applied to the yield segment FA must be statically equivalent to the forces transmitted across the real elastic-plastic interface Γ. The vertical component of the resultant is not known, but, as we noted earlier, the shear stress τ_{xy} vanishes identically on the centerline of the real plastic region so the horizontal component is zero. The statement in terms of the tangential loads is

$$\sum_{k=1}^{M} q_k(\cos \beta_k - 1) = 0 \tag{25}$$

Equation (24) can be added to the last condition to cancel the term -1 in the parentheses.

It is also necessary to determine the contributions of the tangential loads to the vertical displacement and slope at the point F. However, detailed calculations show that if the tangential loads satisfy conditions (24) and (25) then the vertical displacement is identically zero on the stress free portions of the edge of the slit. The discontinuities at the ends of the loaded arcs have been excluded from the elastic region by starting each of the step loads inside the yield segment FA, that is,

$$\beta_1 < \alpha_1 \text{ for } k \geq 1$$
$$\alpha_j < \alpha_1 \text{ for } j \geq 2 \qquad (26)$$

Therefore, the addition of the tangential loads does not modify the conditions (15) and (16) which give zero opening and slope at the point F.

V YIELD CONDITIONS AT POINTS F' AND A

It is also useful to introduce a reference stress Y_t for the tangential loads. Then the dimensionless form of the tangential load coefficients and corresponding stress components are

$$d_k = \frac{q_k}{Y_t} \tag{27}$$

$$S_{xt} + S_{yt} \equiv \frac{\sigma_x + \sigma_y}{Y_t} = \frac{2}{\pi} \sum_{k=1}^{M} d_k \, \mathrm{Re}\{L_{58k}\} \tag{28}$$

$$S_{yt} - S_{xt} + i2T_{xyt} \equiv \frac{\sigma_y - \sigma_x + i2\tau_{xy}}{Y_t} = \frac{1}{\pi} \sum_{k=1}^{M} d_k \left\{ -2L_{58k} + \frac{\zeta}{\zeta^2 - 1} \left[\zeta\left(\bar{\zeta} + \frac{1}{\bar{\zeta}}\right) - \zeta^2 - 1 \right] L'_{58k} \right\} \tag{29}$$

Similar dimensionless forms for stresses due to the normal loads are given in equations (A13) and (A14) of the Appendix. The total stresses are obtained by addition of the components due to normal loads and to tangential loads. Each of the dimensionless forms must be multiplied by the corresponding reference stress Y_n or Y_t and added. The total stresses are

$$\sigma_x = Y_n S_{xn} + Y_t S_{xt}$$

$$\sigma_y = Y_n S_{yn} + Y_t S_{yt} + T = Y_n S_{yn} + Y_t S_{yt} + Y_n \frac{2}{\pi} \sum_{j=1}^{N} c_j \alpha_j \tag{30}$$

$$\tau_{xy} = Y_n T_{xyn} + Y_t T_{xyt}$$

Another condition will now be imposed to obtain the proper shape for the elastic-plastic interface Γ. The slope of that curve must be zero at point A as is indicated in Fig. 1. That is, the derivative of the yield

condition (19) with respect to x must be zero at point A or

$$\left.\frac{\partial f}{\partial x}\right|_A = (2\sigma_x - \sigma_y)\frac{\partial \sigma_x}{\partial x} + (2\sigma_y - \sigma_x)\frac{\partial \sigma_y}{\partial x} + 6\tau_{xy}\left.\frac{\partial \tau_{xy}}{\partial x}\right|_A = 0 \qquad (31)$$

Many of these derivatives are zero since most stress components are constant on the edge of the slit near point A. For all three types of loading the shear stress is zero at A and the normal stress on the end of the slit is constant so $\frac{\partial \sigma_y}{\partial x} = 0$. Also, as we noted before, the components σ_x and σ_y are equal on the slit for the case of normal loads so $\frac{\partial \sigma_x}{\partial x}$ vanishes at A for the normal loads as well as for the simple tension. Hence, condition (31) reduces to the following uncoupled condition on the tangential loads.

$$\left.\frac{\partial \sigma_{xt}}{\partial x}\right|_A = 0 \qquad (32)$$

Reduction of the solution for the tangential loads as ζ tends to a boundary point $e^{i\theta}$ gives the following formula for the stress component σ_{xt} on the slit.

$$\sigma_{xt} = -Y_t \frac{2}{\pi} \sum_{k=1}^{M} d_k \ln\left|\sin^2\theta - \sin^2\beta_k\right| \qquad (33)$$

Therefore, equation (32) will be fulfilled if the coefficients d_k also satisfy the condition

$$\sum_{k=1}^{M} \frac{d_k}{\sin^2\beta_k} = 0 \qquad (34)$$

Now the coefficients d_k have been selected so that the condition (31) is fulfilled, and the c_j have been chosen so that condition (15) and (16)

on slope and displacement at point F are satisfied. The total stress field given by equations (30) must now be adjusted so that the yield condition (19) is satisfied at both point A and at point F. At point F most stress components vanish and we obtain

$$\tau_{xyF} = \sigma_{yF} = 0$$

$$\sigma_{xF} = \sigma_{xnF} + \sigma_{xtF} = -\frac{2}{\pi} Y_n \sum_{j=1}^{N} c_j \alpha_j - \frac{2}{\pi} Y_t \sum_{k=1}^{M} d_k \ln \left| \sin^2 \alpha_1 - \sin^2 \beta_k \right| \tag{35}$$

The stress components at point A are:

$$\tau_{xyA} = 0$$

$$\sigma_{yA} = \sigma_{ynA} + \sigma_{ytA} + T = Y_n \sum_{j=0}^{N} c_j + 0 + \frac{2}{\pi} Y_n \sum_{j=1}^{N} c_j \alpha_j \tag{36}$$

$$\sigma_{xA} = \sigma_{xnA} + \sigma_{xtA} = Y_n \sum_{j=0}^{N} c_j - Y_t \frac{2}{\pi} \sum_{k=1}^{M} d_k \ln \sin^2 \beta_k$$

The coefficients c_j and d_k are known so substituting the stress components at F, given in equation (35), and the stress state at A, given by equations (36) into the yield condition gives two equations which can be solved for the two reference stresses Y_n and Y_t in terms of the yield stress Y_s. Actually two roots are obtained from a quadratic equation, and the one solution is chosen which gives yielding in tension at the point F.

VI DISCUSSION OF NUMERICAL EXAMPLES

An Algol program was written for the evaluation of the stress and displacement components of the basic normal and tangential problems at an arbitrary point in the z-plane. A complex translator which has been developed at Stanford Research Institute simplified the coding of the complex functions.

The weights c_j and d_k are chosen for each step load so that conditions (9), (15), (16), (24), (25), and (34) are satisfied. Then the reference stresses Y_n and Y_t are calculated in terms of the yield stress Y_s so that the yield condition is satisfied at points F and A.

Next, a ray θ = constant is chosen in the ζ-plane and computations of stresses and displacements are made for values of $|\zeta|$ ranging from .01 to 1.0. The corresponding points in the z-plane lie on a hyperbola, and they approach the slit as $|\zeta| \to 1$. A simple iterative scheme is used to find the point on the hyperbola where the yield condition (19) is satisfied. These are points on the elastic-plastic interface, and they are shown by dots in examples of Figures 6, and 7.

In the center of those diagrams are shown the corresponding displacements of the real crack surface. The distribution of normal loads is shown on the right hand yield segment and the tangential loads are sketched on the left yield segment. Both distributions of loads and the opening of the crack are plotted with adjusted vertical scales, but the dots on the interface Γ are plotted with equal vertical and horizontal scales.

VII CONCLUSIONS AND SUGGESTIONS FOR FURTHER WORK

We have seen here that the discontinuity of tranverse displacement and the shear strain at the point F in the Dugdale model can be eliminated by the proper distribution of normal loads. Introduction of the additional tangential loads on the segment FA permits satisfaction of the yield condition at both points F and A. Some of the sample calculations subjected to these restrictions result in an elastic-plastic interface which resembles the experimentally determined curves shown in Forman's report and sketched approximately in Fig. 1. Of course there is still considerable freedom in the choice of the distribution of loads, so we should not yet expect good agreement.

Further work will include attempts to introduce a simple but reasonable work-hardening model for the material inside the curve Γ. This will provide a simple relationship between stresses and displacements in the interior and on the edge Γ of the plastic zone.

Compatability of the elastic and plastic regions will be enforced on the interface Γ. A program for increasing the applied tension T and, consequently the size of the yield zone will be developed. As the load is increased the distribution of stresses and strains in the plastic zone will be studied to attempt to define a failure criterion.

APPENDIX A

THE COMPLEX POTENTIALS FOR STEP NORMAL AND TANGENTIAL LOADS

The case of generalized plane stress in an infinite elastic plane subjected to arbitrary loads on an elliptical boundary can be solved by complex variable methods which are described in the books by Muskhelishvili and Sokolnikoff. The notation of the latter book will be used here.

The mapping function (3) transforms the exterior of the ellipse in the z-plane into the interior of the unit circle in the ζ-plane. Boundary conditions are expressed by the integral

$$F(s) = i\int_{s_0}^{s}(T_x+iT_y)ds = \int_{z_0}^{z}[-p(z')+iq(z')]dz' \qquad (A1)$$

where s is arc length on the boundary curve C in the z-plane, and T_x and T_y are respectively the horizontal and vertical components of boundary forces per unit of arc length for a plate of unit thickness. Note that positive p corresponds to a compressive normal stress on C and positive q corresponds to a negative shear stress. Therefore $p(z') = +p_j$ on the two loaded arcs for the normal case, Fig. 4, and is zero elsewhere. However, $q(z') = +q_k$ on the loaded arcs in the first and third quadrants and $q(z') = -q_k$ in the second and fourth quadrants of the z-plane, Fig. 5.

If the lower limit of integration s_0 is chosen to be the value corresponding to the point E, then the integral for the normal loading gives

$$F(s) = -p_j\begin{cases} z-z_j, & \text{for } z \text{ on arc } z_j, A, \bar{z}_j \\ \bar{z}_j-z_j, & " \quad \bar{z}_j, B, -z_j \\ \bar{z}_j+z, & " \quad -z_j, D, -\bar{z}_j \\ 0 & " \quad -\bar{z}_j, E, z_j \end{cases} \qquad (A2)$$

The transformation to the corresponding boundary point σ in the ζ-plane is simply

$$F^{\circ}(\sigma) = F(s) \tag{A3}$$

where z is replaced by the function $\omega(\zeta)$ in equations (A2). Then the first complex potential $\varphi^{\circ}(\zeta)$ is obtained from the following integral taken around the boundary γ of the unit circle.

$$\varphi^{\circ}(\zeta) = \frac{1}{2\pi i} \oint_{\gamma} F^{\circ}(\sigma) \left[\frac{1}{\sigma-\zeta} - \frac{1}{\sigma} \right] d\sigma \tag{A4}$$

For the simple loading considered here the function $\varphi^{\circ}(\zeta)$ can be expressed in terms of elementary integrals including the function $\ln(\sigma-\zeta)$. The integral must vary continuously as σ transverses the various arcs of γ which determines the branch of the logarithm function and establishes the bounds on the imaginary parts of L_{1j} and L_{2j} given in equations (6). Finally the ellipse is flattened to a slit so that $m \to 1$ and $\bar{z}_j \to z_j$, and we find

$$\varphi^{\circ}(\zeta) = - \frac{p_j}{2\pi i} \left\{ z(\zeta) L_{4j} - \frac{4Ri\alpha_j}{\zeta} - z_j L_{3j} \right\} \tag{A5}$$

The second complex potential is calculated from the relation

$$\psi^{\circ}(\zeta) = \frac{\zeta(\zeta^2+1)}{1-\zeta^2} \frac{d\varphi^{\circ}(\zeta)}{d\zeta} + \frac{1}{2\pi i} \oint_{\gamma} \frac{\overline{F^{\circ}(\sigma)}}{\sigma-\zeta} d\sigma \tag{A6}$$

Several terms can be cancelled to obtain the following results

$$\frac{d\varphi^{\circ}(\zeta)}{d\zeta} = - \frac{p_j}{2\pi i} \left\{ R \frac{\zeta^2-1}{\zeta^2} L_{4j} + \frac{R}{\zeta^2} 4i\alpha_j \right\} \tag{A7}$$

$$\psi^{\circ}(\zeta) = - \frac{p_j}{2\pi i} \left\{ R \frac{\zeta}{1-\zeta^2} 8i\alpha_j - z_j L_{3j} \right\} \tag{A8}$$

The following formulae are given by Sokolnikoff for the stress and displacement components in the z-plane.

$$\sigma_x + \sigma_y = 4\mathrm{Re}\,\frac{d\varphi(z)}{dz} \tag{A9}$$

$$\sigma_y - \sigma_x + i2\tau_{xy} = 2\left[\bar{z}\,\frac{d^2\varphi(z)}{dz^2} + \frac{d\psi(z)}{dz}\right] \tag{A10}$$

$$2\mu(u-iv) = \kappa\,\overline{\varphi(z)} - \bar{z}\,\frac{d\varphi(z)}{dz} - \psi(z) \tag{A11}$$

where $\kappa = \frac{3-\upsilon}{1+\upsilon}$ for generalized plane stress. The complex potentials at corresponding points in the z- and ζ-planes are given by

$$\varphi(z) \equiv \varphi^{o}(\zeta) \qquad \psi(z) \equiv \psi^{o}(\zeta) \tag{A12}$$

Chain differentiation and the mapping function (3) can be used to relate derivatives at corresponding points in the two planes.

Equations (4a) and (4b) express the components of stress due to a single normal load. If the dimensionless load coefficients c_j are introduced and the finiteness condition (9) is used then the dimensionless forms of displacements and stresses due to all the steps of normal load are

$$S_{xn} + S_{yn} = \frac{\sigma_x+\sigma_y}{Y_n} = \frac{2}{\pi}\sum_{j=0}^{N} c_j\,\mathrm{Im}\{L_{4j}(\zeta)\} \tag{A13}$$

$$S_{yn} - S_{xn} + i2T_{xyn} = \frac{\sigma_y-\sigma_x+i2\tau_{xy}}{Y_n} \tag{A14}$$

$$= -\frac{i}{\pi}\,\frac{\zeta^2}{\zeta^2-1}\left\{\left(\bar{\zeta} + \frac{1}{\bar{\zeta}}\right)\sum_{j=0}^{N} c_j\,L'_{4j}(\zeta) - \sum_{j=0}^{N}\frac{c_j z_j}{R}\,L'_{3j}(\zeta)\right\}$$

$$U_n - iV_n = \frac{2\mu}{Y_n}\,\frac{u-iv}{R} \tag{A15}$$

$$= \frac{1}{2\pi i}\left\{-\left(\bar{\zeta} + \frac{1}{\bar{\zeta}}\right)\left[\kappa\sum_{0}^{N} c_j\,\overline{L_{4j}} + \sum_{0}^{N} c_j\,L_{4j}\right] + \kappa\sum_{0}^{N} c_j\,\frac{z_j}{R}\,\overline{L_{3j}} + \sum_{0}^{N} c_j\,\frac{z_j}{R}\,L_{3j}\right\}$$

Letting ζ tend to a boundary point $e^{i\theta}$ on the unit circle, see Fig. 4, and extracting the contribution of the j^{th} step to the sums in (A15) gives the

expression (11) for the displacement on the slit.

The case of the fundamental step in shear loads sketched in Fig. 5 can be solved in a similar manner. However, the tangential load q changes from $+q_k$ to $-q_k$ at points A and D of the boundary which approximately doubles the amount of detailed calculations. The potentials can be reduced to the following forms for a single step load.

$$\varphi^{o}(\zeta) = \frac{q_k}{2\pi}\left\{R(\zeta + \frac{1}{\zeta})L_{58k} - z_k[L_{910k} - i2\pi] + 4R[L_{11k} - i\pi]\right\} \qquad (A16)$$

$$\psi^{o}(\zeta) = \frac{-q_k}{2\pi}\left\{2R(\zeta + \frac{1}{\zeta})L_{58k} - z_k L_{910k} + 4RL_{11k}\right\} \qquad (A17)$$

where the abbreviations are

$$L_{58k} \equiv L_{5k} - L_{6k} + L_{7k} - L_{8k} \qquad L_{910k} \equiv L_{9k} + L_{10k}$$

$$L_{5k} \equiv \ln\frac{1-\zeta}{\sigma_k-\zeta} \qquad L_{6k} \equiv \ln\frac{\bar{\sigma}_k-\zeta}{1-\zeta}$$

$$L_{7k} \equiv \ln\frac{-1-\zeta}{-\sigma_k-\zeta} \qquad L_{8k} \equiv \ln\frac{-\bar{\sigma}_k-\zeta}{-1-\zeta} \qquad (A18)$$

$$L_{9k} \equiv \ln\frac{-\bar{\sigma}_k-\zeta}{\sigma_k-\zeta} \qquad L_{10k} \equiv \ln\frac{-\sigma_k-\zeta}{\bar{\sigma}_k-\zeta}$$

$$L_{11k} \equiv \ln\frac{-1-\zeta}{1-\zeta}$$

The imaginary parts of each of the functions L_{5k} to L_{11k} also lie in the interval 0 to 2π. The positive angles marked in Fig. 5 represent the imaginary parts of the first four functions L_{5k} to L_{8k}.

Further straightforward, but tedious, calculations lead to the dimensionless stresses in equation (28) and (29) due to all of the step tangential loads. The corresponding dimensionless displacements are

$$U_t - iV_t \equiv \frac{2\mu}{Y_t}\frac{u-iv}{R} = \frac{1}{2\pi}\left\{ \kappa\left[(\bar{\zeta}+\frac{1}{\bar{\zeta}})\overline{S_1} - \overline{S_3} + 4\overline{S_4}\right] + \left[2(\zeta+\frac{1}{\zeta}) - (\bar{\zeta}+\frac{1}{\bar{\zeta}})\right]S_1 - S_3 + 4S_4 \right\} \tag{A19}$$

where the new sums are

$$S_1 \equiv \sum_{k=1}^{M} d_k L_{58k} \qquad S_2 \equiv \sum_{k=1}^{M} d_k \frac{d}{d\zeta} L_{58k}$$

$$S_3 \equiv \sum_{k=1}^{M} \frac{z_k}{R} d_k L_{910k} \qquad S_4 \equiv \sum_{k=1}^{M} d_k L_{11k} \tag{A20}$$

REFERENCES

1. Griffith, A. A., "The Phenomenon of Rupture and Flow in Solids," Phil. Trans. Roy. Soc., A221, 1920, pp. 163-198.

2. Inglis, C. E., "Stresses in a Plate due to the Presence of Cracks and Sharp Corners," Trans. Inst. Nav. Arch., 55, 1913, pp. 219-230.

3. Zheltov, Yu. P., and Khristianovitch, S. A., "On the Mechanism of Hydraulic Fracture of an Oil-Bearing Stratum," Izvestiya AN SSSR, OTN, 5, 1955, pp. 3-41, (in Russian).

4. Barenblatt, G. I., "On the Equilibrium Cracks due to Brittle Fracture," Doklady AN SSR, 127, 1959, pp. 47-50, (in Russian).

5. Dugdale, D. S., "Yielding of Steel Sheets Containing Slits," J. Mech. Phys. Solids, 8, 1960, pp. 100-104.

6. Rosenfield, A. R., Dai, P. K., and Hahn, G. T., "Crack Extension and Propagation Under Plane Stress," Proceedings of the First International Conference on Fracture, Sendai, Japan, 1965, pp. A179-A226.

7. Forman, R. G., "Experimental Program to Determine Effect of Crack Buckling and Specimen Dimensions on Fracture Toughness of Thin Sheet Materials," Wright-Patterson AFB, Tech. Rept. AFFDL-TR-65-146, January, 1966.

8. Goodier, J. N., and Field, F. A., "Plastic Energy Dissipation in Crack Propagation," Fracture of Solids, Wiley, New York, 1962.

9. Muskhelishvili, N. I., Some Basic Problems of the Mathematical Theory of Elasticity, Noordhoff, Groningen-Holland, 1953.

10. Sokolnikoff, I. S., Mathematical Theory of Elasticity, McGraw-Hill, New York, 1956.

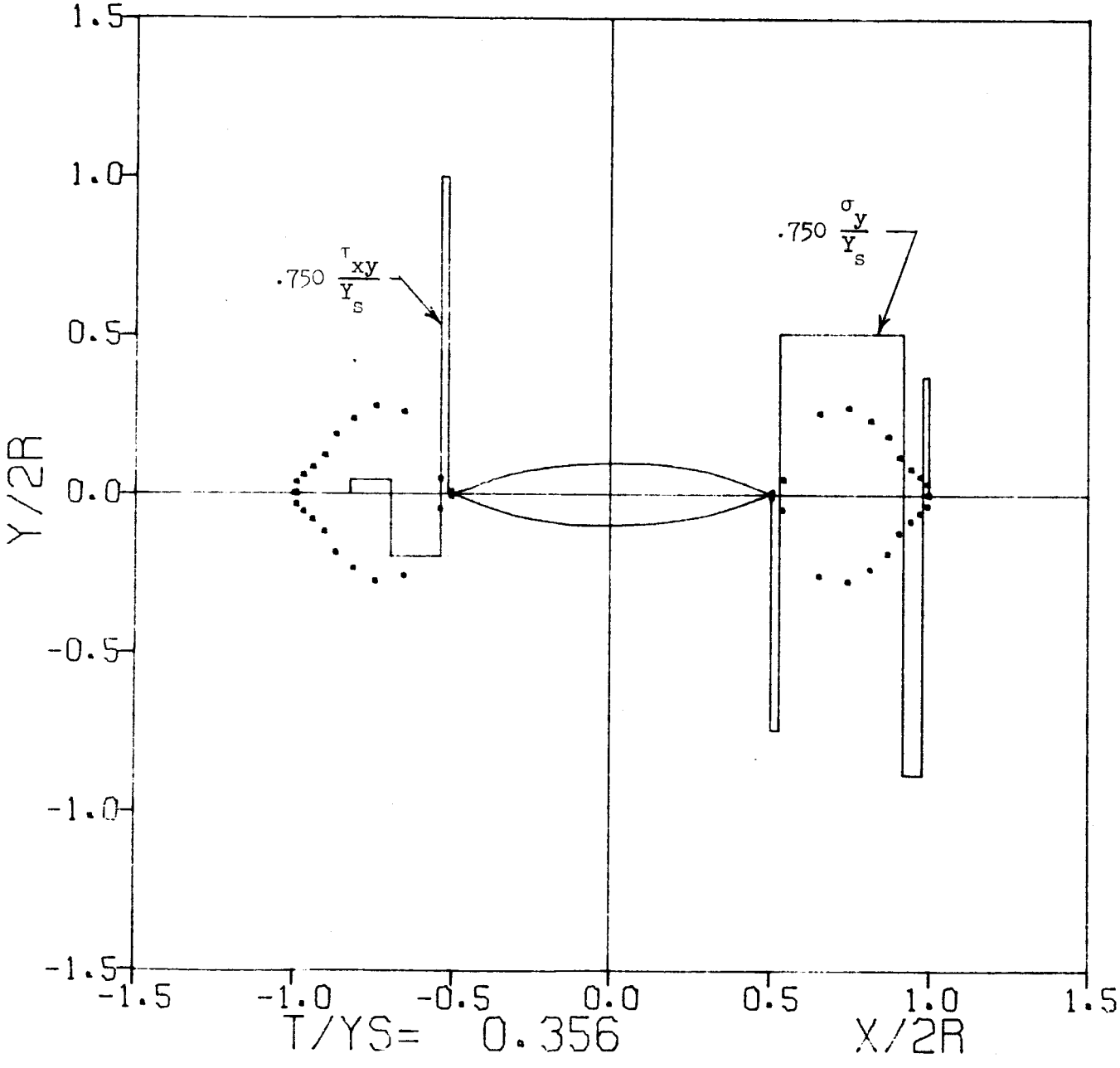

Fig. 6

AN EXAMPLE OF STEP DISTRIBUTIONS OF NORMAL AND TANGENTIAL LOAD. THE DOTS REPRESENT POINTS ON THE ELASTIC-PLASTIC INTERFACE. CRACK OPENING IS SHOWN WITH AN EXAGGERATED SCALE.

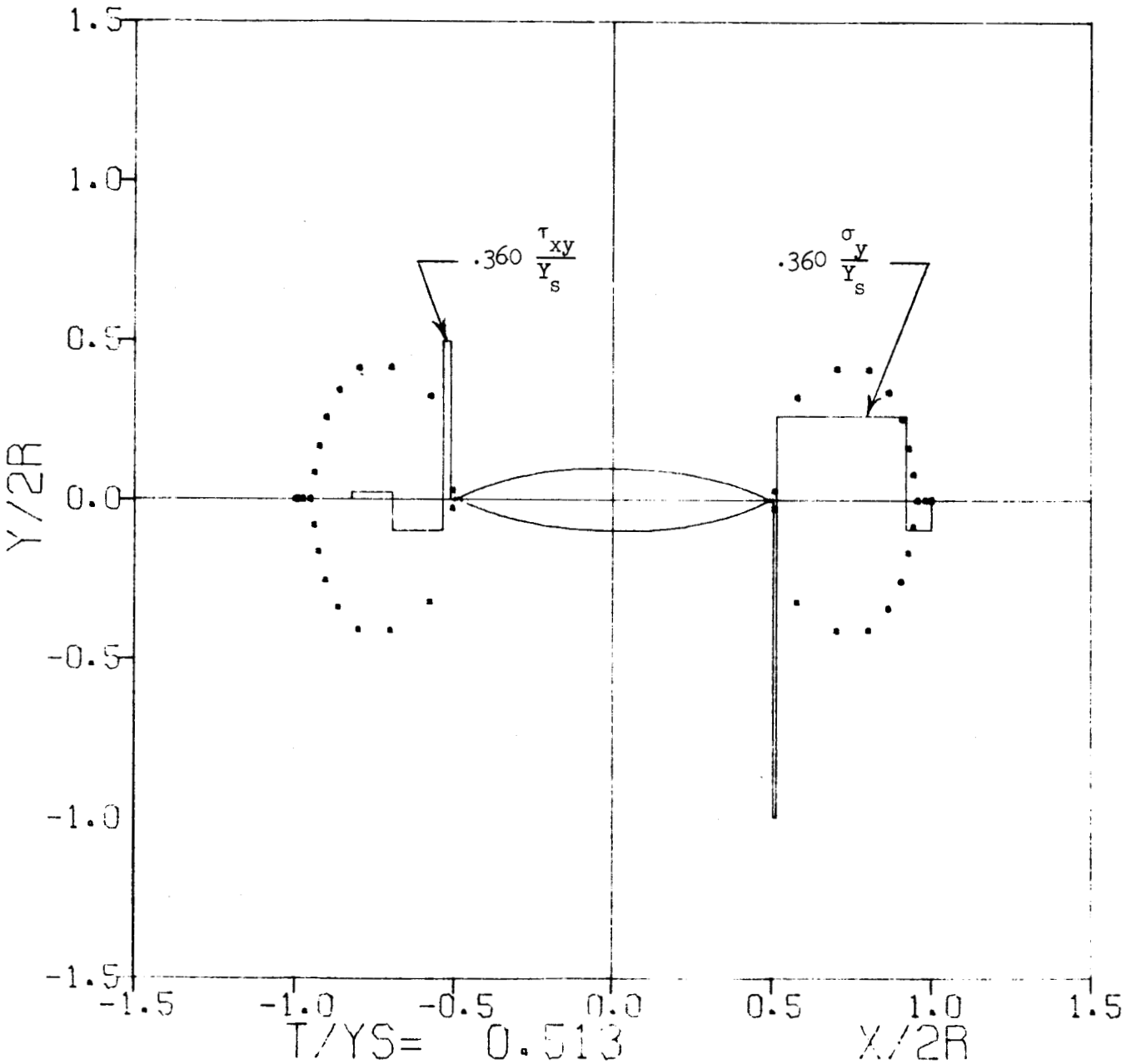

Fig. 7

AN EXAMPLE OF STEP DISTRIBUTIONS OF NORMAL AND TANGENTIAL LOAD. THE DOTS REPRESENT POINTS ON THE ELASTIC-PLASTIC INTERFACE. CRACK OPENING IS SHOWN WITH AN EXAGGERATED SCALE.

DISTRIBUTION LIST

NAS1-5885

	Copies
NASA Langley Research Center Langley Station Hampton, Virginia 23365	
Attention: Contracting Officer, Mail Stop 126	1
Research Reports Division, Mail Stop 122	1
R. L. Zavasky, Mail Stop 117	1
Harvey G. McComb, Jr., Mail Stop 188c	2
NASA Ames Research Center Moffett Field, California 94035	
Attention: Library	1
NASA Flight Research Center P. O. Box 273 Edwards, California 93523	
Attention: Library	1
NASA Goddard Space Flight Center Greenbelt, Maryland 20771	
Attention: Library	1
Jet Propulsion Laboratory 4800 Grove Drive Pasadena, California 91103	
Attention: Library	1
NASA Manned Spacecraft Center 2101 Webster Seabrook Road Houston, Texas 77058	
Attention: Library	1
NASA Marshall Space Flight Center Huntsville, Alabama 35812	
Attention: Library	1
NASA Western Operations 150 Pico Boulevard Santa Monica, California 90406	
Attention: Library	1
NASA Wallops Station Wallops Island, Virginia 23337	
Attention: Library	1
NASA Electronics Research Center 575 Technology Square Cambridge, Massachusetts 02139	
Attention: Library	1

DISTRIBUTION LIST

NAS1-5885

	Copies	
NASA Lewis Research Center 21000 Brookpark Road Cleveland, Ohio 44135 Attention: Library, Mail Stop 3-7	1	
NASA John F. Kennedy Space Center Kennedy Space Center, Florida 32899 Attention: Code ATS-132	1	
NASA Michoud Assembly Facility P. O. Box 26078 New Orleans, Louisiana 70126 Attention: Code I-Mich-D	1	
National Aeronautics and Space Administration Washington, D.C. 20546 Attention: Library, Code USS-10 NASA Code RA	1 1	
NASA Scientific and Technical Information Facility P. O. Box 33 College Park, Maryland 20740	56	plus reproducible